

**The Clusters AgeS Experiment (CASE):  
Variable Stars in the Globular Cluster 47 Tucanae<sup>1</sup>**J. Kaluzny<sup>1</sup>, M. Rożyczka<sup>1</sup>, W. Pych<sup>1</sup>, W. Krzeminski<sup>1</sup>,  
K. Złoczewski<sup>1</sup>, W. Narloch<sup>1</sup> and I. B. Thompson<sup>2</sup><sup>1</sup> Nicolaus Copernicus Astronomical Center, ul. Bartycka 18, 00-716 Warsaw, Poland  
e-mail: (jka, mnr, wojtek, psych, kzlocz, wnarloch)@camk.edu.pl<sup>2</sup> Carnegie Observatories, 813 Santa Barbara Street, Pasadena, CA 91101-1292, USA  
e-mail: ian@obs.carnegiescience.edu*Received June 1, 2013***ABSTRACT**

Based on over 5400 *BV* images of 47 Tuc collected between 1998 and 2010 we obtained light curves of 65 variables, 21 of which are newly detected objects. New variables are located mostly just outside of the core in a region poorly studied by earlier surveys of the cluster. Among them there are four detached eclipsing binaries and five likely optical counterparts of X-ray sources. Two detached systems are promising targets for follow-up observations. We briefly discuss properties of the most interesting new variables.

**Key words:** *globular clusters: individual: 47 Tuc – blue stragglers – binaries: eclipsing – stars: variables*

**1. Introduction**

47 Tuc (NGC 104), one of the brightest and most massive Milky Way's globular clusters (GC), is located about 4.5 kpc away from the Sun at a high galactic latitude of  $-44.9$  deg (Harris 1996, 2010 edition). With a core radius of  $0'.36$  and a half-light radius of  $3'.17$ , it had long been suspected to be on the verge of core-collapse; however recent simulations of Giersz & Heggie (2011) suggest that the collapse may not take place for another  $\sim 25$  Gyr. In either case, the very central region of 47 Tuc is inaccessible to the photometry with ground-based telescopes lacking adaptive optics. The outer parts of the cluster, up to a radius of about  $\sim 22'$ , can be observed rather easily, the only obstacle being the contamination by stars from the outskirts of the Small Magellanic Cloud.

---

<sup>1</sup>Based on data obtained at Las Campanas Observatory using the 6.5 m Magellan Clay Telescope and the Swope 1.0 m Telescope.

Early photometric studies of 47 Tuc led to the detection of a number of pulsating variables (Fox 1982 and references therein). An early spectroscopic search for binary stars (Mayor et al. 1984) yielded a negative result: no such objects were found among 64 stars located farther than 5 core radii from the cluster center, "indicating a lower binary frequency and/or different distribution of orbital parameters than in field stars in the solar neighborhood". The first binaries in 47 Tuc (two W UMa type and six detached or semidetached systems) were identified based on the HST-WFPC1 time-series photometry of cluster's core by Edmonds et al. (1996). Another two W UMas were found by Kaluzny et al. (1997). A more extensive survey of Kaluzny et al. (1998) resulted in the detection of 42 variables, among which there were 12 eclipsing binaries (nine W UMas and three detached/semi-detached systems).

Using HST-WFPC2, Albrow et al. (2001) derived a time series photometry for over 46,000 main-sequence stars in the core of 47 Tuc. Among them they found 11 detached eclipsing binaries, 15 W UMas, 10 contact or near-contact non-eclipsing systems, and 71 variables with nearly sinusoidal to clearly non-sinusoidal light curves and periods ranging from 0.4 to 10 d, which they classified as BY Dra stars rotating synchronously with unseen companions. Six of the latter were located far to the right of the cluster's main sequence (MS), prompting the authors to define a new class of GC members which they proposed to call red stragglers. An extensive ground-based survey by Weldrake et al. (2004) led to the detection of 69 new variables, more than doubling the number of such objects in the 47 Tuc field. About 70% of the newly identified variables belonged to SMC.

One of the new detections of Weldrake et al. (2004) – the detached eclipsing binary V69 – was subject to a detailed photometric and spectroscopic analysis performed by Thompson et al. (2010). They derived absolute parameters of its components with an accuracy better than 1%, estimated its age using mass-luminosity-age, mass-radius-age, and (turnoff mass)-age relations, and determined the helium abundance  $Y$  with an accuracy of 0.03 for each of the components. Having at least one detached eclipsing binary (DEB) more would enable a more accurate direct determination of  $Y$  for 47 Tuc. This exciting possibility caused us to embark on an extensive survey aimed at the detection of new DEBs in outer parts of 47 Tuc (note that objects located in the outskirts of the cluster are only suitable for the ground-based high-resolution optical spectroscopy).

Section 2 contains a brief report on the observations and explains the methods used to calibrate the photometry. Variables (both the newly detected and the known ones) identified during our survey are described in Section 3. A summary of the paper is contained in Section 4.

## 2. Observations and Photometric Reductions

The cluster was observed at Las Campanas Observatory on the 1.0-m Swope telescope equipped with the  $2048 \times 3150$  pixel SITe3 camera. Two overlapping fields with the size  $14'.45$  by  $22'.84$  (henceforth referred to as E and W) were covered. The longer axis of each field was oriented N-S. The overlap region extended over  $1'.58$  in RA, so that the effectively observed composite field had a size of  $27'.32$  by  $22'.84$ . The composite field was centered on the core of 47 Tuc. All the images were obtained with the same set of  $BV$  filters at a scale of  $0.435$  arcsec/pixel. Those taken at a seeing in excess of  $3$  arcsec were not included in the present analysis.

The bulk of observations were collected during two long runs (43 nights in total) in 2009 and 2010. We obtained then 2879 useful frames in  $V$  and 344 in  $B$  at a median seeing of  $1.5$  and  $1.6$  arcsec, respectively, with average exposures of  $117$  s for  $V$  and  $193$  s for  $B$ . The exposure time of a given frame depended on the momentary seeing, and was adjusted so as to keep the level of saturation constant (i.e. to maintain the same magnitude of the brightest unsaturated stars). The data collected in 2009 – 2010 were supplemented with a set of images obtained between 1998 and 2008 which comprised of 1337  $V$ - and 400  $B$ -frames of field E together with 371  $V$ - and 95  $B$ -frames of field W. A part of that set was subrastered to  $14'.45$  by  $15'.6$ . The images had the same quality as those collected in 2009 – 2010.

The light curves of detected stars were extracted with the image subtraction package DIAPL.<sup>2</sup> Daophot, Allstar and Daogrow codes (Stetson 1987, 1990) were used to extract the profile photometry of point sources and to derive aperture corrections for reference images. The reference images in  $V$  were made from 47 and 50 individual frames of fields E and W with an average seeing of  $1.15$  and  $1.11$  arcsec, respectively, while those in  $B$  were made from 15 and 22 images, respectively, with an average seeing  $1.29$  in both E and W.

For the analysis, the E and W fields were divided into  $4 \times 6$  segments to reduce the effects of PSF variability. The light curves derived with DIAPL were converted from differential counts to magnitudes based on profile photometry and aperture corrections determined for each segment of reference images separately. Instrumental magnitudes were transformed to the standard  $BV$  system as described in Section 2.1. The  $V$ -band light curves were extracted for 63024 sources in field E and 52591 sources in field W. Accounting for the overlap, we obtained 110141 unique light curves in the whole composite field.

In Fig. 1 the  $rms$  values of individual measurements in  $V$  are plotted versus the average  $V$ -magnitude for each object in field W. The photometric accuracy reaches about  $3$  mmag at  $V = 14.0$  mag, decreasing to  $\sim 10$  mmag for the turnoff stars at  $V = 17.0$  mag and to  $\sim 100$  mmag at the faintest stars for which the measurement

<sup>2</sup>Freely accessible at <http://users.camk.edu.pl/pych/DIAPL/index.html>

could still be performed ( $V = 20.5$  mag). Exactly the same accuracy was reached in field E. Stars with  $V < 13.0$  mag were overexposed on the reference images of both fields, making the study of their light curves impossible. Depending on exposure time and seeing, some images of stars with  $13 < V < 13.5$  mag were also saturated. Their light curves were filtered to remove points affected by saturation.

### 2.1. Calibration

The instrumental magnitudes for reference images were converted to the standard ones using linear transformations based on 817 and 570 local Stetson's standards in fields W and E, respectively (Stetson 2000; 2009 on-line version). The following transformations were derived:

$$\begin{aligned} v &= V - 0.086(3) \times (B - V) - 1.591(3) \\ b &= B - 0.146(4) \times (B - V) - 2.054(4) \\ b - v &= 0.938(3) \times (B - V) - 0.462(3) \end{aligned} \quad (1)$$

(field E) and

$$\begin{aligned} v &= V - 0.074(3) \times (B - V) - 1.602(3) \\ b &= B - 0.139(4) \times (B - V) - 2.038(4) \\ b - v &= 0.936(3) \times (B - V) - 0.437(3) \end{aligned} \quad (2)$$

(field W), where capital letters denote the standard magnitudes.

As most of the monitoring was conducted in  $V$  only, the standard magnitudes were derived using average values of  $B - V$ . This introduced some systematic errors in the case of color-changing objects. However, for most of the variables the amplitude of color variations did not exceed 0.1 mag, and the systematic error of  $V$  magnitude was smaller than 0.01 mag. For the main goal of our survey, which is to detect new variables, inaccuracies of this size are unimportant.

The astrometric solutions for the reference images in  $V$  were found based on positions of 2997 UCAC3 stars (Zacharias et al. 2010). The average residuals in RA and DEC between cataloged and recovered coordinates amount to 0.14 and 0.14 arcsec, respectively. For the detection of variables we used methods described in Kaluzny et al. (2013). A total of 65 variables were found (among them 21 new ones). They are listed in Table 1 along with their equatorial coordinates and cross-identifications for catalogs published by Weldrake et al. (2004), Kaluzny et al. (1998) and Samus et al. (2009). We detected variability of all but one object from Weldrake et al. (2004) present in the surveyed field (our photometry shows no brightness variations for their star V93).

Finding charts for newly detected variables are shown in Fig. 2.

### 3. Variables

The basic properties of variables detected in our survey are listed in Table 2. The periods in column 2 were derived with the method employing periodic orthogonal polynomials to fit the observations and the analysis of variance statistic to evaluate the quality of the fit (Schwarzenberg-Czerny 1996), as implemented in the TATRY code kindly made available by the author.

The parameter  $\Delta V$  listed in column 4 gives the full range of the measured  $V$ -magnitude, including seasonal changes of light curves. The last column of Table 2 contains the proposed classification of variables, with “new” indicating newly detected objects. EW, EB and EA denote eclipsing binaries with light curves of W UMa,  $\beta$  Lyrae and Algol type, respectively; Ell stands for ellipsoidal variables, and stars located along or near the red giant branch on the cluster color-magnitude diagram (CMD) are labeled with RGB. The variability of the latter is likely caused by ellipsoidal effect and/or chromospheric activity related to binarity. Among the new variables there are five likely optical counterparts to X-ray sources detected with the Chandra telescope by Heinke et al. (2005).

Figure 3 presents the CMD of a small section of the monitored field with marked locations of all but two variables listed in Tables 1 and 2. Not included are W26 and E20 - very red Miras with  $B - V > 3$  mag which were originally detected by the OGLE group (Soszynski et al. 2009). The group of variables located to the blue of the cluster’s main sequence at  $V \approx 19$  is composed of RR Lyr pulsators from the SMC. The sequence of red long period variables starting at ( $V \approx 19$ ,  $B - V \approx 1.1$ ) and extending to  $B - V \approx 2.0$  also consists of SMC stars. Fig. 4 shows the positions in the cluster CMD of a selection of our variables, including all eclipsing binaries and three particularly interesting objects which will be discussed below. Phased light curves for 14 new variables are displayed in Fig. 5 (not shown are RR-Lyrae stars, long period variables, and E32 whose period is not known). Light curves for all 65 variables detected within the present survey can be found in the electronic version of this paper available from the Acta Astronomica archive of from CASE archive at <http://case.camk.edu.pl>.

#### 3.1. Eclipsing binaries

The main result of our survey is the detection of four new detached eclipsing binaries. All these objects are located beyond the core region of the cluster and are suitable for spectroscopic follow-up studies with ground-based telescopes.

The light curve of W12 shows a shallow secondary eclipse with  $\Delta V \approx 0.1$  mag and a primary eclipse with  $\Delta V \approx 0.4$  mag. A preliminary solution of the  $V$ -light curve indicates a high luminosity ratio of the components:  $L_p/L_s = 9$ . The expected luminosity ratio for the  $I$  band equals to 6, so that the near-IR spectroscopy may allow for the determination of radial velocity curves of both components.

The available light curve of E32 shows only one clear eclipse with  $\Delta V = 0.6$  mag. This means that the orbital period has to be longer than 10 days (and may

**Table 1:** Equatorial coordinates of variable stars identified within the present survey

ID	RA <sub>J2000</sub> [deg]	Dec <sub>J2000</sub> [deg]	ID-W <sup>a</sup>	ID-K <sup>b</sup>	ID-S <sup>c</sup>	ID	RA <sub>J2000</sub> [deg]	Dec <sub>J2000</sub> [deg]	ID-W <sup>a</sup>	ID-K <sup>b</sup>	ID-S <sup>c</sup>
W1	6.04262	-72.06708				E9	6.45689	-71.97410	V99	226	
W2	5.91532	-72.02788				E10	6.55163	-72.03701	V27	230	
W3	6.05276	-72.11105			V001	E11	6.51274	-72.05086	V28	229	
W4	6.02083	-72.08958				E12	6.38434	-72.03098	V100	225	V044
W5	5.99704	-72.11350				E13	6.53692	-72.11706	V7	228	V046
W6	5.91897	-72.09997		217	V009	E14	6.42508	-72.10040	V10	223	
W7	5.95557	-72.21893				E15	6.54387	-72.18549	V6	227	V045
W8	5.69983	-71.94696				E16	6.53915	-72.20798	V5	255	
W9	5.68282	-71.95575	V71	234		E17	6.39210	-72.16616	V9	222	
W10	5.77913	-72.02260		218		E18	6.51177	-72.24155			
W11	5.84984	-72.05125				E19	6.40987	-72.23572			
W12	5.73147	-72.08756				E20	6.40448	-72.25761		252	
W13	5.72354	-72.06296	V69			E21	6.31753	-71.93490	V30	238	V047
W14	5.65323	-72.11997				E22	6.24824	-71.89658		241	
W15	5.81761	-72.18639				E23	6.20544	-71.93885	V34		
W16	5.77493	-72.15847	V97			E24	6.25194	-72.00076	V32	221	V043
W17	5.67023	-72.15625	V96	215		E25	6.17727	-72.10601			
W18	5.69786	-72.22143	V95	245	V050	E26	6.17207	-72.10331			
W19	5.63677	-71.99193	V70	216		E27	6.29647	-72.20400	V14	250	V052
W20	5.54779	-71.98831	V62			E28	6.27575	-72.17319	V15	219	
W21	5.50268	-72.03445	V61	214	V042	E29	6.15076	-71.95535	V33	239	
W22	5.46433	-72.18055	V91			E30	6.17717	-71.98994	V31	220	
W23	5.63907	-72.23045	V94	246		E31	6.05647	-71.96737			
W24	5.27715	-71.94372	V64			E32	6.15633	-72.06476			
W25	5.34974	-72.25939	V92	243		E33	6.07805	-72.08192			
W26	5.27031	-72.25646		242		E34	6.04263	-72.06709			
E1	6.75007	-71.91918	V26			E35	6.10767	-72.11765			
E2	6.69230	-71.99538				E36	6.09773	-72.14155	V17		
E3	6.73688	-72.17036	V13	232		E37	6.09675	-72.12296			
E4	6.69681	-72.27622				E38	6.07745	-72.13304			V002
E5	6.67914	-72.25578	V12	253	V053	E39	6.02089	-72.08958			
E6	6.58064	-72.23394	V4	254		E40	6.13241	-72.15819	V16	251	
E7	6.40631	-71.93440	V29			E41	6.10552	-72.22732			
E8	6.51136	-71.97276		231							

<sup>a</sup> Weldrake et al. 2004; <sup>b</sup> Kaluzny et al. 1988; <sup>c</sup> Samus et al. 2009

be significantly longer). We obtained a single spectrum of E32 with the MIKE Echelle spectrograph on the 6.5 m Magellan Clay telescope, and we found that the binary is an SB2 system. Several additional spectra are needed to establish the ephemeris with confidence. This in turn will enable further photometric observations in eclipses, and finally the determination of absolute parameters of the system. The location of E32 on the CMD indicates that at least one of its components is an evolved star at or past the turnoff. The analysis of E32 together with V69 (Thompson et al. 2010) may allow interesting limits to be placed on the helium abundance of 47 Tuc.

For W7 we have three MIKE/Magellan spectra. They show that the variable is an SB1 binary with measured velocities of  $-37.41 \pm 0.32$ ,  $-74.27 \pm 0.22$  and  $+16.38 \pm 0.16$  km/s at orbital phases 0.49 (HJD 245 5769.866), 0.353 (HJD 245 5770.839) and 0.692 (HJD 55836.642), respectively. These measurements indicate that the binary is a likely member of the cluster. The systemic velocity of 47 Tuc

is equal to -18.0 km/s, and the velocity dispersion at the location of W7 amounts to  $\sim 11$  km/s (Harris 1996). This can be compared with the binary's velocity near conjunction at orbital phase 0.49. The fourth detached system, E39, is placed rather far from the cluster main sequence and may be a foreground halo object. Its low luminosity and short orbital period make it a difficult target for spectroscopy.

**Table 2:** Properties of variable stars identified within the present survey

ID	P [d]	$V_{max}$ [mag]	$\Delta V$ [mag]	$< B - V >$	Type of variability Remarks
W1	0.36115544(1)	15.607	0.163	0.600	EW, YS, <b>new</b> , Ch-0024410.2-720401 <sup>a</sup>
W2	0.28287568(1)	17.565	0.317	0.543	EW, <b>new</b>
W3	-	11.753	2.872	1.516	LP
W4	0.35298992(1)	15.838	0.163	0.271	EW, BS, <b>new</b> , Ch-002404.9-720522
W5	0.28036018(8)	17.143	0.225	0.420	EW, BS, <b>new</b> , Ch-002359.3-720648
W6	0.73703372(1)	13.063	1.024	0.261	RR
W7	3.88255(2)	19.091	0.384	0.815	EA, <b>new</b>
W8	12.78227(2)	14.150	0.032	1.173	Ell?, RGB, <b>new</b>
W9	0.6158898(1)	19.084	0.811	0.439	RR
W10	-	15.976	0.384	1.652	LP
W11	0.63228616(9)	18.948	0.184	1.145	RR, <b>new</b>
W12	3.732001(2)	17.462	0.411	0.634	EA, <b>new</b>
W13	29.53975(1)	16.799	0.616	0.537	EA
W14	0.04595852(3)	14.679	0.037	0.145	SX, BS, <b>new</b>
W15	71.4156(5)	17.138	0.141	1.557	LP, <b>new</b>
W16	0.39708061(4)	18.859	0.274	0.834	EB
W17	8.4278094(1)	16.638	0.203	0.931	?
W18	0.27890017(1)	15.459	0.424	0.565	EW, YS
W19	0.36164588(6)	19.584	0.624	0.276	RR
W20	66.6	16.991	0.611	1.792	LPO066 <sup>b</sup>
W21	0.273741797(2)	17.919	0.360	0.610	EW
W22	0.65390427(7)	18.738	0.264	0.582	RR, blend?
W23	0.57218584(4)	19.017	0.980	0.428	RR
W24	0.595771(2)	19.323	0.839	0.301	RR
W25	0.6256305(15)	19.364	0.752	0.404	RR
W26	269.3	16.879	1.406	3.347	LPO015
E1	0.347489131(4)	17.025	0.485	0.493	EW, BS
E2	0.8102273(2)	18.306	0.168	0.734	RR, <b>new</b>
E3	0.36349524(3)	19.129	0.733	0.240	RR
E4	79.92	16.850	0.297	2.053	LPO446
E5	0.44625922(1)	16.659	0.398	0.434	EB, BS
E6	-	16.539	0.254	1.783	LP
E7	4.463003(6)	18.792	0.210	1.273	?
E8	6.371513(8)	14.141	0.152	0.760	RGB-clump
E9	0.64752185(2)	18.959	0.852	0.446	RR
E10	4.78667(2)	17.474	0.603	0.917	?
E11	8.3711839(8)	14.916	0.157	0.911	RGB
E12	0.234635701(3)	19.441	0.787	0.981	EW
E13	1.150686034(3)	15.797	0.417	0.233	EB, BS
E14	0.29712114(1)	17.306	0.505	0.238	RR

Continued on next page

Table 2 – continued from previous page

ID	P [d]	$V_{max}$ [mag]	$\Delta V$ [mag]	$< B - V >$ [mag]	Type of variability Remarks
E15	0.378854028(1)	16.397	0.311	0.349	EW, BS
E16	0.52515175(1)	18.977	1.254	0.422	RR
E17	20.791(1)	16.576	0.207	0.733	RGB
E18	14.09425(2)	17.176	0.070	1.405	?, <b>new</b>
E19	-	14.344	0.194	0.989	LP, <b>new</b>
E20	266.4	17.911	2.254	3.607	LPO329
E21	0.250546155(3)	18.397	0.457	0.669	EW
E22	35.3519(1)	16.747	0.111	1.680	LP
E23	0.24169575(1)	18.551	0.337	0.693	EW
E24	0.313434596(1)	17.650	0.519	0.511	EW
E25	3.33587(4)	17.849	0.143	0.589	?, <b>new</b>
E26	1.4043996(8)	18.528	0.282	1.276	?, <b>new</b>
E27	0.351384786(1)	16.244	0.246	0.318	EW, BS
E28	36.8914(12)	15.252	0.148	0.900	RGB
E29	40.39(16)	16.613	0.111	1.608	LP
E30	10.77526(2)	16.007	0.320	0.814	RGB
E31	20.43463(6)	16.564	0.457	0.901	RGB, <b>new</b>
E32	-	17.109	0.362	0.569	EA, <b>new</b>
E33	0.25151879(1)	16.391	0.107	1.044	Ell?, <b>new</b> , Ch-002418.6-720455
E34	9.87379(4)	15.495	0.294	0.878	RGB, <b>new</b> , Ch-002425.8-720703
E35	0.300361921(7)	18.021	0.345	0.648	EW
E36	0.279869331(2)	18.053	0.641	0.703	EW, <b>new</b>
E37	135.43559(2)	13.180	2.480	1.301	LP
E38	3.480885(3)	16.468	0.313	0.843	RGB
E39	0.987519(2)	18.792	0.507	0.937	EA, <b>new</b>

<sup>a</sup> Ch - optical counterpart of a Chandra X-ray source from Heinke et al. (2005)

<sup>b</sup> LPO - OGLE long period variable (Soszynski et al. 2009)

In addition to the five detached binaries our sample includes one semi-detached system (E13; Kaluzny et al. 2007) and 15 contact or nearly-contact binaries. Six of them are blue stragglers, and two (W1 and W18) are located in the region occupied by yellow stragglers (see e.g. Stetson 1994). Variable yellow stragglers are rare objects and therefore we examined HST/ACS images of W1 and W18 to check whether or not the ground based photometry is affected by blending. We found W18 to be an isolated object with no indication for unresolved visual companions on ACS images. Still, we cannot rule out the possibility that it is a triple system like many (perhaps most) W UMa stars (Rucinski et al 2007). Spectroscopic observations can clarify this issue. As for W1, ACS images show three visual components forming a blend which cannot be resolved on our ground based images. Two closest components of the blend are separated by 0.3 arcsec. Thus, based on the available evidence, W1 cannot be regarded as a yellow straggler.

### 3.2. Notes on individual objects

Some of the newly detected variables deserve a short comment on their properties. The red straggler candidate E33 is located only 61 arcsec away from the



cluster centre; however it is an isolated object whose ground based photometry is free from blending-related problems. This was confirmed by the examination of HST/ACS/F625W images. The star has a sine-like light curve with  $\Delta V = 0.11$  mag and a period of 0.25 d which was coherent and stable during several observing seasons between 1998 and 2010. This indicates that the observed variability is very likely related to the binarity of E33. We have tentatively classified E33 as an ellipsoidal variable. Heinke et al. (2005) analyzed two sets of Chandra data for 47 Tuc. The X-ray counterpart of E33 was detected in 2002 with an X-ray luminosity of  $0.7E30$  erg/s in 0.5-2.5 keV band, but no X-rays were detected at E33 position in 2000. This implies a seasonal variability of the X-ray source connected with the star. The variable is too red to be an ordinary contact binary regardless of its membership status in 47 Tuc. This is evident by comparing its color with colors of contact systems E21 and E23 whose orbital periods are similar to the period of E33 (see Fig. 4). As for the membership status of E33, the examination of stacked subtracted images from seasons 1998, 1998, 2009, and 2010 does not indicate any proper motion with respect to cluster stars. The qualitative method we used to estimate the proper motion is based on Eyer and Wozniak (2001). Spectroscopic data are needed to clarify the evolutionary and membership status of E33.

The variable E8 is located on the red horizontal branch on the cluster CMD. The light curve shows coherent changes with  $\Delta V = 0.15$  mag and  $P = 6.4$  d. The amplitude of the light curve exhibits small but easily visible seasonal changes. Similar variations with the same period were detected by the OGLE group in 1993 (Kaluzny et al. 1998). Given the coherence of the variability it is likely that the star is a binary. If so, it would be a rare example of a photometrically variable binary from the red horizontal branch. With  $P = 6.4$  d and a radius of the red giant component of about  $10 R_{\odot}$ , E8 would have to be a rather compact system. Obviously, if the variability was induced mainly by the ellipsoidal effect, the actual orbital period of a binary would double to 12.8 d. The bright blue straggler W14 turned out to be an SX Phe-type pulsator. It is the first such variable detected in 47 Tuc. SX Phe stars are common among blue stragglers in metal-poor globular clusters, but rather rare in metal rich ones.

Finally, we note the presence of several variables located on or slightly to the red of the red giant branch of the cluster, newly detected of which are E31 and E34 (see Figs. 3 and 4). They are good candidates for binaries and are easy targets for a spectroscopic follow-up.

#### 4. Summary

We performed a photometric study of the globular cluster 47 Tuc with a time baseline of more than ten years. Based on over 6500 *BV* frames we have identified 65 variable stars, 21 of which are new detections. We provide celestial coordinates of all variables, and cross-identifications of the variables discovered earlier by other

authors. Finding charts for the new variables are also provided. Five of the new variables are likely optical counterparts of X-ray sources, and another four ones are detached eclipsing binaries. Two detached eclipsing systems are located close to the main-sequence turnoff on the CMD of 47 Tuc, and we argue that they are promising targets for detailed photometric and spectroscopic studies: when combined with the results of an earlier study of W13 (Thompson et al. 2010; their variable V69) they may allow an improved constraint on the helium content of the cluster. The yellow straggler W18, the red straggler E33 and the red horizontal branch object E8 are another systems deserving further study which would clarify their membership and evolutionary status.

**Acknowledgements.** JK, MNR, WP and WN were partly supported by the grant NCN 2012/05/B/ST9/03931 from the Polish Ministry of Science.

## REFERENCES

- Albrow, M. D., Gilliland, R. L., Brown, T. M., Edmonds, P. D., Guhathakurta, P., Sarajedini, A. 2001, *ApJ*, **559**, 1060.
- Clark, L. L., Sandquist, E. L., Bolte, M. 2004, *AJ*, **128**, 3019.
- Edmonds, P. D., Gilliland, R. L., Guhathakurta, P., Petro, D. P., Saha, A., Shara, M. M. 1996, *ApJ*, **468**, 241.
- Eyer, L., Wozniak, P. R. 2001, *MNRAS*, **327**, 601.
- Fox, M. W. 1982, *MNRAS*, **199**, 715.
- Giersz, M., Heggie, D. C. 2011, *MNRAS*, **410**, 2698.
- Harris, W.E. 1996, *AJ*, **112**, 1487.
- Heinke, C. O., et al. 2005, *ApJ*, **625**, 796.
- Mayor, M., Imbert, M., Andersen, J., Ardeberg, A., Benz, W. et al. 1984, *A&A*, **134**, 118.
- Kaluzny, J., Krzeminski, W., Mazur, B., Wysocka, A., Stepień, K. 1997, *Acta Astron.*, **47**, 249.
- Kaluzny, J., Kubiak, M., Szymanski, M., Udalski, A., Krzeminski, W., Mateo, M., Stanek, K. Z. 1998, *A&A Suppl.*, **128**, 19.
- Kaluzny, J., Thompson, I. B., Rucinski, S. M., Pych, W., Stachowski, G., Krzeminski, W.; Burley, G. S. 2007, *AJ*, **134**, 541.
- Samus, N. N., Kazarovets, E. V., Pastukhova, E. N., Tsvetkova, T. M., Durlevich, O. V. 2009, *PASP*, **121**, 1378.
- Schwarzenberg-Czerny, A. 1996, *ApJ*, **460**, 107.
- Soszynski, I., et al. 2009, *Acta Astron.*, **59**, 239.
- Stetson, P. B. 1987, *PASP*, **99**, 191.
- Stetson, P. B. 1990, *PASP*, **102**, 932.
- Stetson, P. B. 1994, *PASP*, **106**, 250.
- Stetson, P. B. 2000, *PASP*, **112**, 925.
- Thompson, I. B., et. al 2010, *AJ*, **139**, 329.
- Weldrake, D. T. F., Sackett, P. D., Bridges, T. J., Freeman, K. C. 2004, *AJ*, **128**, 736.
- Zacharias, N., Finch, C., Girard, T., Hambly, N., Wycoff, G., et al. 2010, *AJ*, **139**, 2184.

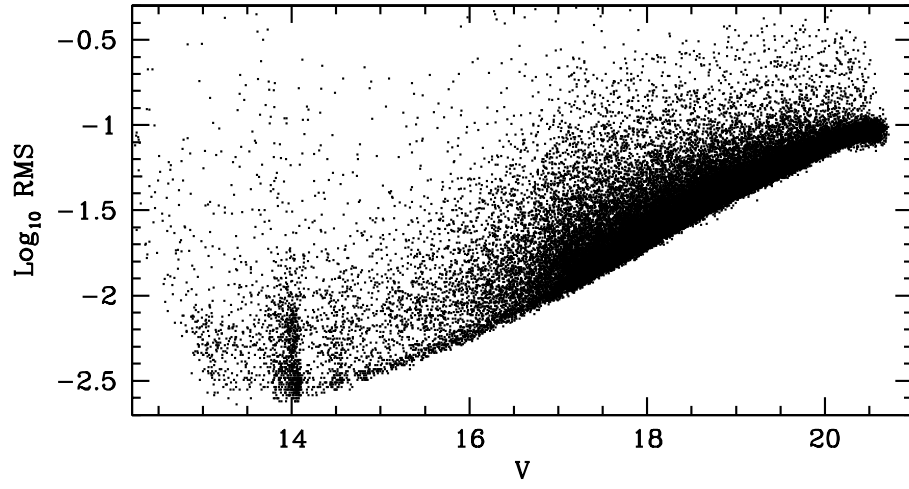


**Figure 1:** The accuracy of the photometry of 47 Tuc. For each object in field W the *RMS* values of individual measurements in the *V*-band are plotted vs. the average *V*-magnitude.

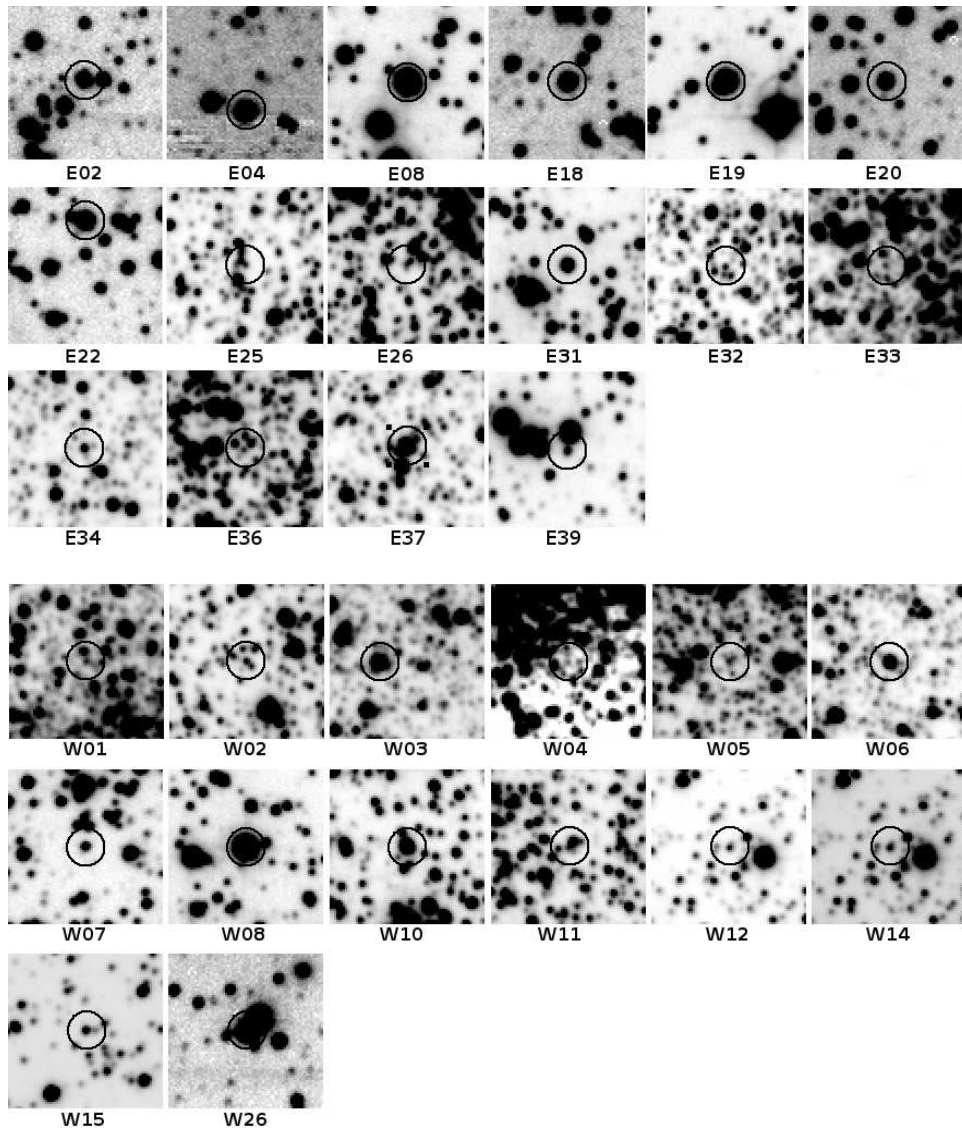


**Figure 2:** Finding charts for the newly detected variables. Each chart is 30 arcsec on a side, with north up and east to the left.

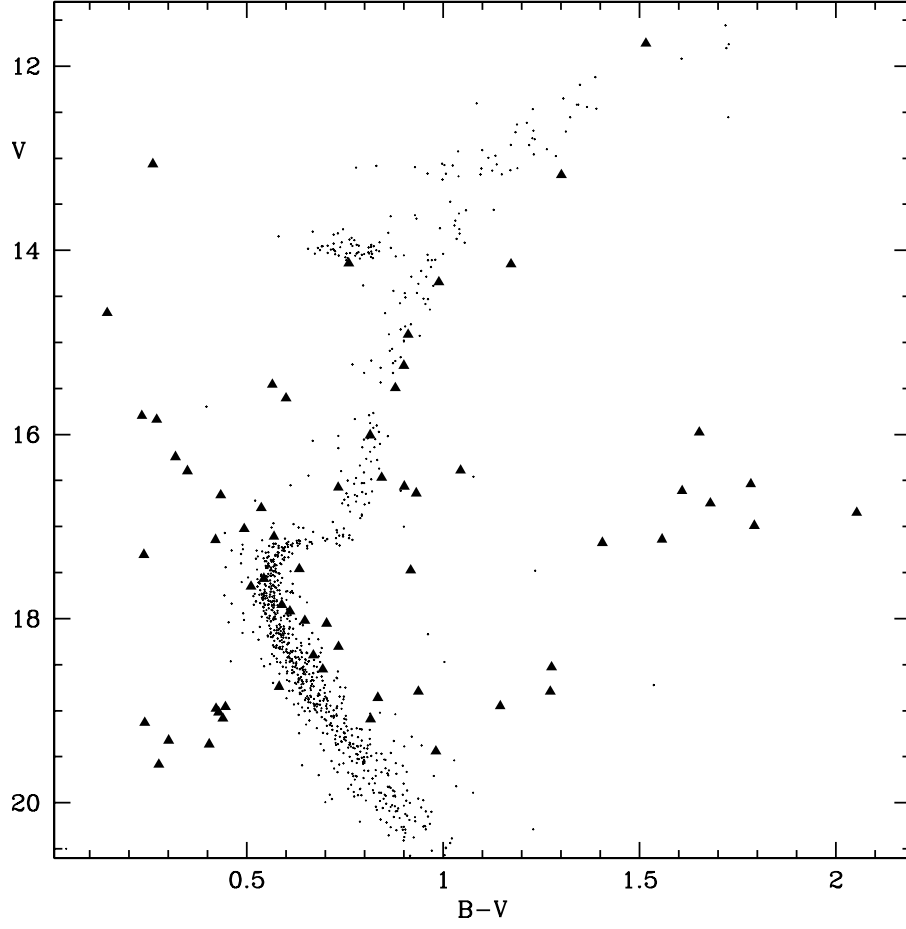


**Figure 3:** CMD of 47 Tuc with positions of 63 variables detected by the CASE program marked with triangles. Not shown are two very red Miras with  $B - V > 3$ , detected earlier by the OGLE group (Soszynski et al. 2009). Background dots: nonvariable stars selected from a small fragment of the observed field.

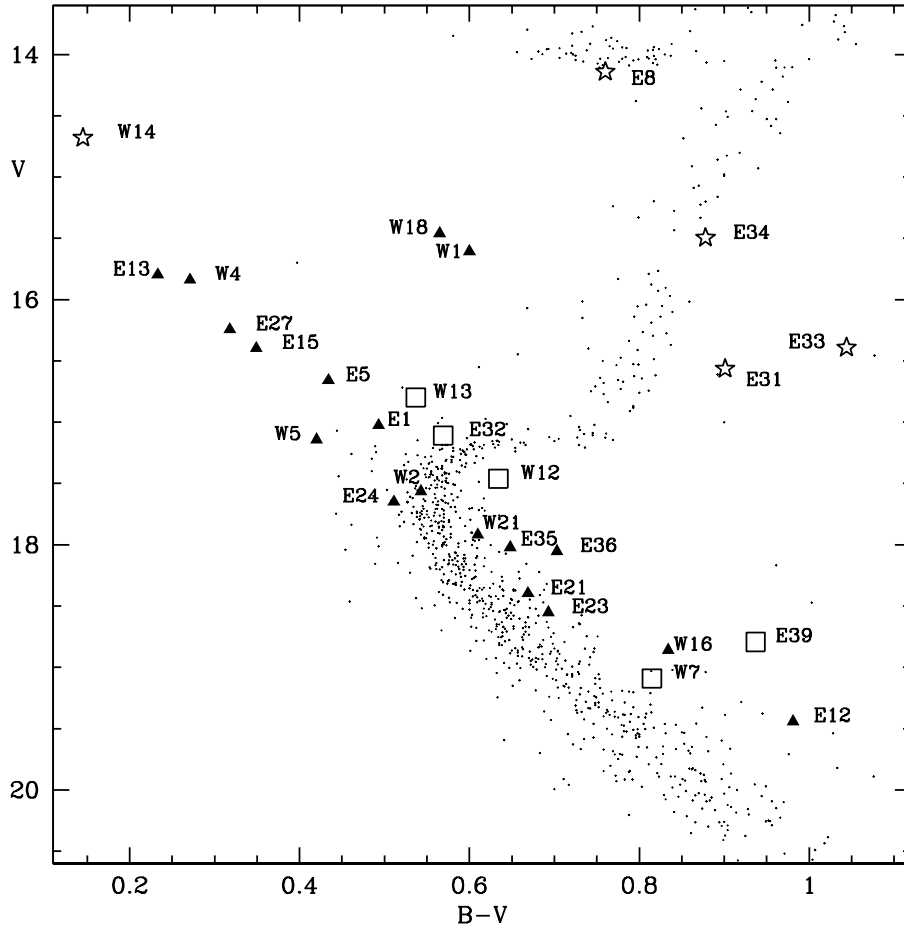


**Figure 4:** CMD of 47 Tuc with positions of all binaries detected by the CASE program. Also shown are a few other variables briefly discussed in Section 3.2. Squares: detached binaries; triangles: contact binaries; stars: other variables. Background dots: nonvariable stars selected from a small fragment of the observed field.

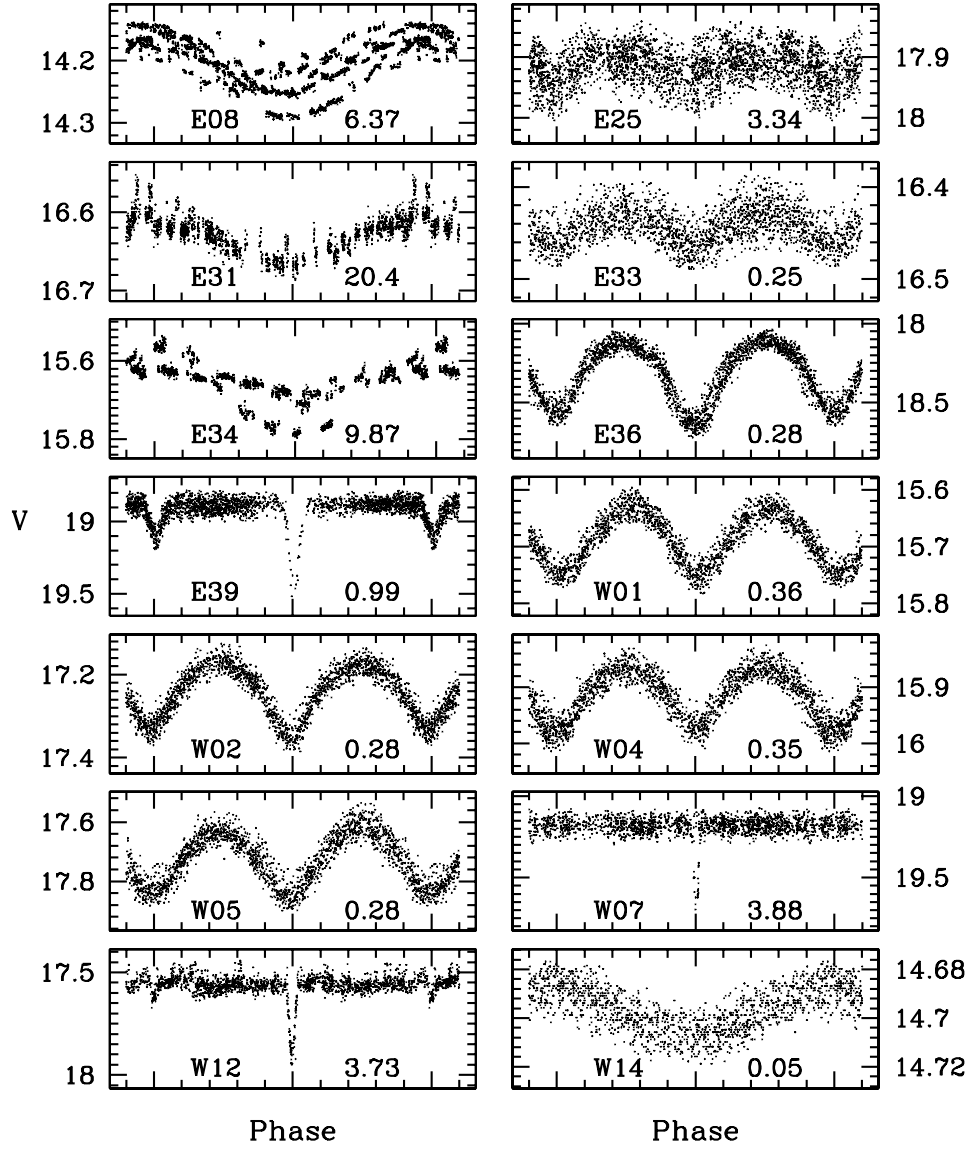


**Figure 5:** Phased  $V$ -light curves of newly detected eclipsing binaries and a few new variables of other types. In each panel the left label gives the name of the variable, and the right label the orbital period in days.